The Effect of Axonal "Beading" on Water Diffusion Properties: A Monte Carlo Simulation of Axonal Degeneration and its Effects on DTI Contrasts

J. A. Farrell[1,2], B. A. Landman[3], J. Zhang[2], S. Smith[1,2], D. S. Reich[4,5], P. A. Calabresi[5], and P. C. van Zijl[1,2]

[1]F.M. Kirby Research Center for Functional Brain Imaging, Kennedy Krieger Institute, Baltimore, Maryland, United States, [2]Neuroscience Section, Division of MR Research, Dept. of Radiology, Johns Hopkins University School of Medicine, Baltimore, Maryland, United States, [3]Dept. of Biomedical Engineering, Johns Hopkins University School of Medicine, Baltimore, Maryland, United States, [4]Division of Neuroradiology, Dept. of Radiology, Johns Hopkins University School of Mediciine, Baltimore, Maryland, United States, [5]Dept. of Neurology, Johns Hopkins University School of Medicine, Baltimore, Maryland, United States

Introduction: Axonal and myelin membranes present barriers to water diffusion. Diffusion Tensor Imaging (DTI) studies of Wallerian degeneration in the optic nerve [1] and traumatic axonal injury [2] have reported a decrease in diffusion parallel to the white matter (WM) fiber, which may be specific to axonal degeneration. Axonal "beading" is characterized by multiple localized 1-5μm (radius) dilations of the axonal membrane that resemble "beads on a string" [3] and has been reported after axonal transection [4,5], and in multiple sclerosis [6]. Understanding the relationship between axonal morphology and the diffusion weighted imaging (DWI) signal is therefore a vital step in the development and validation of DTI methodology to study WM damage. This study employs Monte Carlo simulations to investigate the effect of axonal "beading" on diffusion. Previously, diffusion in the interstitial space of synthetic fiber phantoms [7] has been simulated with Monte Carlo approaches, and formulas have been presented for diffusion in impermeable cylinders [8] and models of WM fibers [9,10]. Here we demonstrate that axonal "beading" significantly alters diffusion properties and show its effect on the perpendicular and parallel diffusion contrasts currently used to study WM damage.

Methods: The Brownian motion of 100,000 spins was simulated using a Monte Carlo framework [11] that enables the study of diffusion in relevant biological geometries. Simulations were performed on an infinite lattice (i.e. the periodic repetition of a unit cell), where the unit cell contains a healthy axon (represented as an impermeable cylinder), or a degenerating axon (modeled as the union of a cylinder and a sphere). The cylinder radius (R_{cyl}) was 0.5 or 1.5μm, and the sphere radius (R_{sph}) was incremented from 0 to 9μm in steps of 0.5μm. The separation between "beads" on the infinite cylinder was 20μm, consistent with histology [5,6]. Spins were assigned random initial positions within the geometry. A diffusion time of 20ms, time step Δt =1μs, and diffusion constant D = 2μm^2/ms, resulted in a step length $l = 0.110\mu m$ ($l = \sqrt{6D\Delta t}$). DWI experiments (PGSE, δ = 3ms, Δ = 21ms, T2 = 100ms) were simulated by computing the phase dispersion over all spins, at several b values, and diffusion weighting gradient orientations. The DTI contrasts of parallel diffusivity ($D_\parallel$), perpendicular diffusivity ($D_\perp$), mean diffusivity (MD) and fractional anisotropy (FA) were computed at b =1000 s/mm^2 assuming an oriented symmetric tensor and Gaussian diffusion. The probability density function (PDF) for diffusion was generated from the histogram of spin displacements, and the kurtosis excess (KE) [12] was computed to determine the deviation from Gaussian diffusion behavior.

Results and Discussion: **Fig. 1** shows four unit cell geometries with increasing R_{sph} for R_{cyl} = 1.5μm. **Fig. 2** shows the effect of "bead" size (increasing R_{sph}) on the signal attenuation and shape of the PDF. ***Perpendicular diffusion:*** The signal attenuation is more pronounced for large R_{sph} and remains mono-exponential over a wide range of b-values. As the 3D root mean square displacement for free diffusion is large (15μm over 20ms) compared to the confining geometry, the PDF for R_{sph}= 0μm agrees with the autocorrelation function (ACF) for cylindrical geometry. As R_{sph} increases, the PDF broadens but remains restricted compared to free diffusion. ***Parallel diffusion:*** For R_{sph} = 0μm, ln(S/S$_0$) falls off rapidly and linearly vs. b, and the PDF approximates free diffusion. As R_{sph} increases, the signal attenuation is diminished and a "bi-exponential" behavior is apparent, which is notable given that the confining geometry is continuous (no distinct physical compartments) and has a single diffusion constant. As R_{sph} increases, the PDF becomes more peaked (less Gaussian). **Fig. 3** Presents the relationship between morphological parameters (R_{cyl}, R_{sph}) and DTI contrasts. As the "bead" size (R_{sph}) increases, $D_\parallel$, MD, and FA decrease, whereas $D_\perp$ increases. Notably, the downward trend of $D_\parallel$ and MD is reversed at $R_{sph} \approx 4$ μm due to the increased spherical volume fraction. The plot of $KE_\parallel$ demonstrates that parallel diffusion is particularly sensitive to changes in morphology and may be near Gaussian (KE ≈ 0) for small and large R_{sph}, but markedly non-Gaussian (KE > 0) at intermediate bead sizes ($R_{sph} \approx 4\mu m$).

Fig 1. Geometries

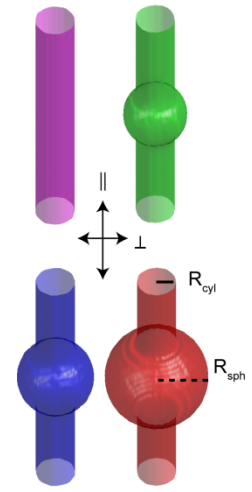

Fig 2. Signal Attenuation and PDFs for R_{cyl} = 1.5 μm

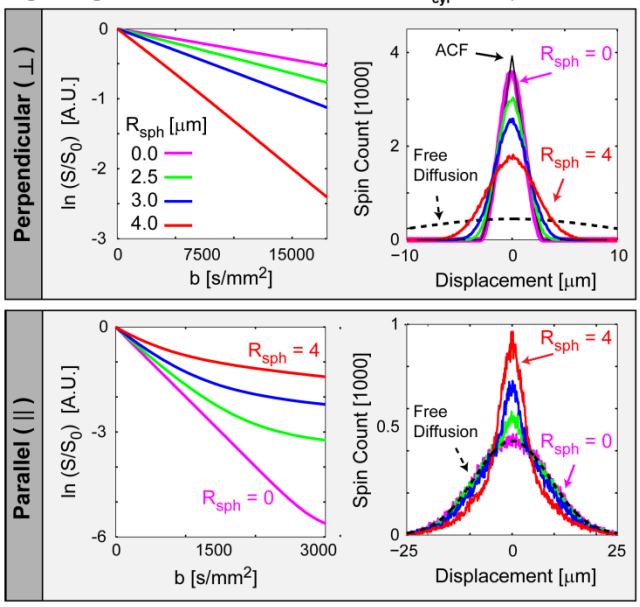

Fig 3. Effect of R_{cyl} and R_{sph} on DTI Contrasts and PDF Properties

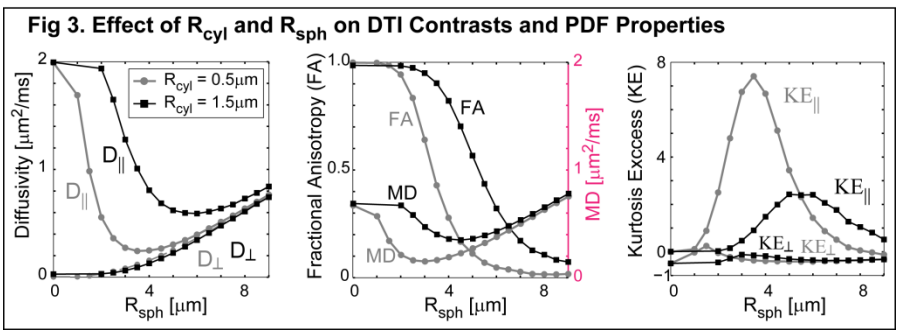

Conclusion: This model examines the effect of axonal "beading" on intracellular diffusion. Beading (in the range of sizes noted in histology, R_{sph} up to ≈ 4 μm), is shown to produce decreased, less-Gaussian, parallel diffusion and increased, more Gaussian, perpendicular diffusion. The exact relationships between axon morphology, diffusion time, and DTI contrasts are complex and require further study. Simulations of diffusion in biologically relevant geometries may aid the interpretation of DWI experiments and advance the development of DWI contrasts specific for axonal injury.

References: [1] Song SK, *et al*, NeuroImage 2003, 20:1714. [2] Mac Donald CL, *et al*, J. Neuroscience 2007, 27(44):11869. [3] Coleman MP, *et al*, J. of Neurological Sciences 2005, 233:133. [4] George R, Griffin JW, J. of Neurocytology 1994, 23:657. [5] Kerschensteiner M, et al, Nature Med., 2005, 11(5):572. [6] Trapp BD, *et al*, New Engl. J. Med. 1998, 338:278. [7] Fieremans E, *et al*, JMR 2008, 190:189. [8] Söderman O, Jönsonn B, JMR(A) 1995, 117:94. [9] Stanisz GJ, *et al*, MRM 1997, 37:103. [10] Pfeuffer J, *et al*, NMR Biomed. 1998, 11:19. [11] Landman B, *et al*, Submitted abstract, ISMRM 2009. [12] Latt J., *et al*, MRI 2008, 26:77. **Funding:** NIH/NCRR-P41RR15241, NMSS CA1029A2, TR3760A3; NIH AG20012; Nancy Davis Center Without Walls.